To: Professor Qi Lu

From: Christopher Jin, Frederic Liu, Gordon Lou, Owen Chen, Yanjun He

Subject: ME1042 Lab 06 Heat Treatment of Materials

Date: June 21, 2023

On 4^{th} and 11^{st} November, Gordon Lou, Owen Chen, Frederic Liu, Yanjun He, and I conducted our sixth experiment in the course Mechanical Measurements 2, from which we have studied the hardness by the Rockwell F scale for several heat-treated metal material samples by several different ways. The types of heat treatment we test are water quenching, vermiculite normalizing and tempering. One without heat treatment sample is used for comparsopm.

For water quenching, the process is to heat the metal material up to the austenite temperature, and maintain until equilibrium. Then quickly remove it from the furnace and place in water to cool it rapidly to the room temperature to form martensite, For vermiculite normalizing, also heat the metal material first up to the austenite temperature until equilibrium, but instead put it into the vermiculite bath then to allow it to cool slowly to form pearlite. For tempering, the forepart procedure is the same as that in water quenching, but after the metal is cooled down, place it into the furnace again to heat up to a certain temperature to improve the metal's brittleness, which known as a tempered martensite.

After measuring the hardness of steel after heat treatment, for which the results are shown in Table 1, we found that the water quenched sample is harder than vermiculite-cooled sample. Because quench will make the steel from austenite to martensite, and martensite is harder than pearlite and bainite which come from annealing or normalizing (vermiculite-cooled). The main reasons for the high hardness of martensite are the solid solution strengthening and grain boundary strengthening of carbon atoms. For solid solution strengthening, interstice atom carbon is in the flat octahedral interstice of the α phase lattice, resulting in a square distortion of the lattice and a stress field. The stress field interacts strongly with dislocation, thus increasing martensite strength. For grain boundary strengthening, the smaller the size of martensite lath or martensite, the higher the martensite strength, because martensite phase boundary hinders dislocation movement, the finer the supercooled austenite grain, the higher the martensite strength. The relatively few slip systems (along which dislocation move) for the BCT structure. For phase transformation strengthening, martensite transformation causes lattice defects with high density in the crystal. Both high density dislocation in lath martensite and twin in lamellar martensite hinder dislocation movement, thus leading to martensite strengthening. For aging strengthening, after the formation of martensite, atoms of carbon and alloy elements diffuse to dislocation or other crystal defects at the segregation or precipitation, pin dislocation, so that dislocation difficult to move, resulting in martensite strengthening.

General speaking, quenching results in large amounts of martensite in steel and it can harden steel. To be more specific, quenching means rapid cooling rate which makes carbon atoms do not have time to diffuse out of the crystal structure in large enough quantities to form cementite (Fe_3C), and then, the austenite (FCC structure) transforms to martensite which has a highly strained body-centered tetragonal form that is supersaturated with carbon. At the same time, the shear deformations during this process lead to a lot of dislocations, and it is a primary strengthening mechanism of steels. Figure 4 gives the micrograph of martensite containing 0.8% carbon. The gray platelike regions are martensite, which have the same composition as the original austenite (white regions). From an experimental standpoint, the most intuitive data is the change in hardness. Martensite can achieve 700 Brinell while the highest hardness of a pearlitic steel is only 400 Brinell (Avallone et al., 2007).

For the steel GB #45, Nunura et al. (2015) tested the hardness of steel without heat treatment and after heat treatment. As a result, without treatment, the hardness of steel is 55 HRC. After normalizing, steel has a hardness of 57 HRC, and after quenching, it has a higher hardness (HRC 58-62). Then after tempering, its hardness is HRC 39. But we found that there is no intersection between the two in the HRC and HRF conversion tables. Instead, we can observe that the trend of the experimental data we made is the same as the experimental data of Nunura et al. (2015).

Our experiment may have the following reasons for the deviation of the experimental data.

The first type of error is caused by the deformation and movement of the iron sheet during the hardness test (Low III et al., 2001). In our experiments, we can observe that when the indenter exerts a certain amount of force on the iron sheet for a certain period of time, the iron sheet will produce a certain amount of deformation, and this amount of deformation will cause the measured hardness to be higher.

The second type of error is caused by the fact that the hardness parameters exceed the specified standard (Asgharzadeh et al., 2020). For the second type of error, the hardness tester needs to be calibrated with a standard block before measurement. For the Rockwell hardness tester calibration results, the difference is qualified within 1. A stable value with a difference within 2 can give a correction value. When the difference is outside the range of 2, the hardness tester must be calibrated and repaired or measured by other hardness testing methods. Each scale of Rockwell hardness has an actual applicable range, which should be selected correctly according to regulations. For example, when the hardness is higher than HRB 100, the HRC scale should be used for testing; when the hardness is lower than HRC 20, the HRB scale should be used for testing. Because the accuracy and sensitivity of the hardness tester is poor when it exceeds the specified test range, and the hardness value is not accurate, it is not suitable for use. Other hardness testing methods also have corresponding calibration standards. The standard block used to calibrate the hardness tester cannot be used on both sides, because the hardness

of the standard surface and the back surface may not be the same. It is generally stipulated that the standard block is valid within one year from the date of calibration. In addition, when replacing the indenter or anvil, pay attention to the contact parts to be wiped clean. After the replacement, test several times with a steel sample with a certain hardness until the hardness value obtained twice in succession is the same. The purpose is to make the contact part of the indenter or anvil and the testing machine be pressed tightly, and the contact is good, so as not to affect the accuracy of the test results.

The third source of error may be that we used too much force when using the loading handle. Before loading, we need to check whether the loading handle is in the unloading position (Barbato et al., 1998). When loading, our action should be light and steady, and we should not use too much force. After loading, the loading handle should be placed in the unloading position to prevent the instrument from being under load for a long time and plastic deformation, which will affect the measurement accuracy.

The fourth type of error may be caused by the bending of the iron sheet after heat treatment (Low et al., 2000). When we polished the iron sheet, we observed that the iron sheet was in a bent state. This leads to the fact that the iron sheet is not fully attached to the platform during the hardness test, so there will be errors in the hardness we measured.

The last type of error may be caused by the decarburization of the iron sheet caused by the heat treatment (Pimenta et al., 2018). We found that there was a black layer on the surface of the iron sheet after heat treatment. Decarburization is likely to occur when the heating temperature of steel is too high or the residence time at high temperature is too long. Sometimes it is accompanied by severe surface oxidation. When the fully decarburized layer appears, there is no pearlite in the tissue. Part of the pearlite remains when there is only a part of the decarburized layer, which leads to the hardness of our measurement is too large.

After this experiment, with observing and comparing the hardness results for the three heat-treated samples, we have learned a lot about the procedure of quenching, normalizing and tempering, and have a better glimpse of the characteristics as well as the application condition for all of the materials, which promotes the theories we have learned in class. In the future, if we have the opportunity to study in the materials science, even in specialty materials field, today's experiment will provide us with tremendous help regarding to this usefulness and significance.

Table 1: Data for steel hardness.

Hardness \ Set	1	2	3	Average
Without heat treatment	71.7	73.6	74.0	73.1
After normalizing	76.6	77.4	74.5	76.2
After quenching	75.8	79.6	82.6	79.3
After tempering	67.6	61.0	65.6	64.7

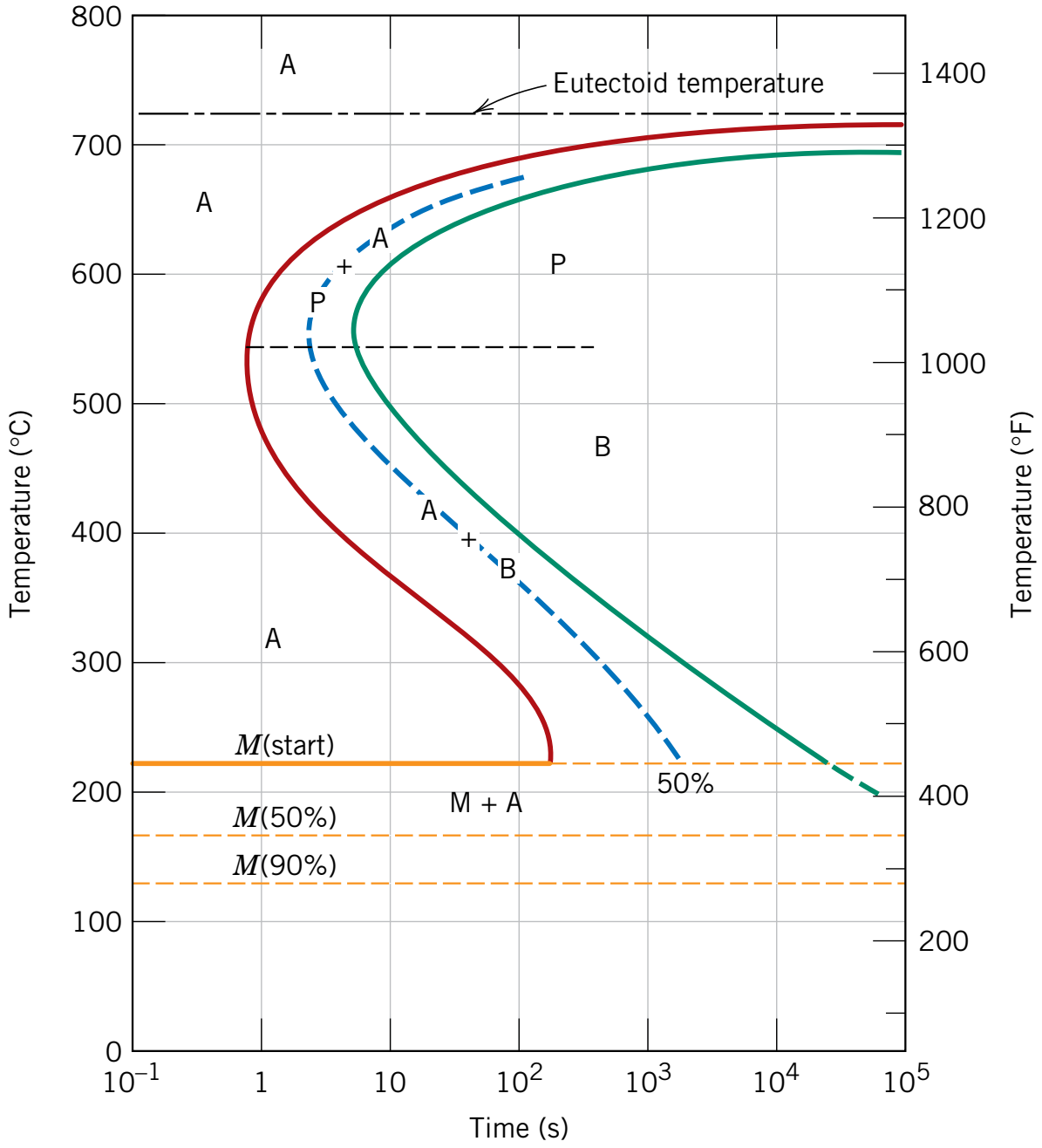

Figure 1: The complete isothermal transformation diagram for an iron–carbon alloy of eutectoid composition: A, austenite; B, bainite; M, martensite; P, pearlite (Callister & Rethwisch, 2018).

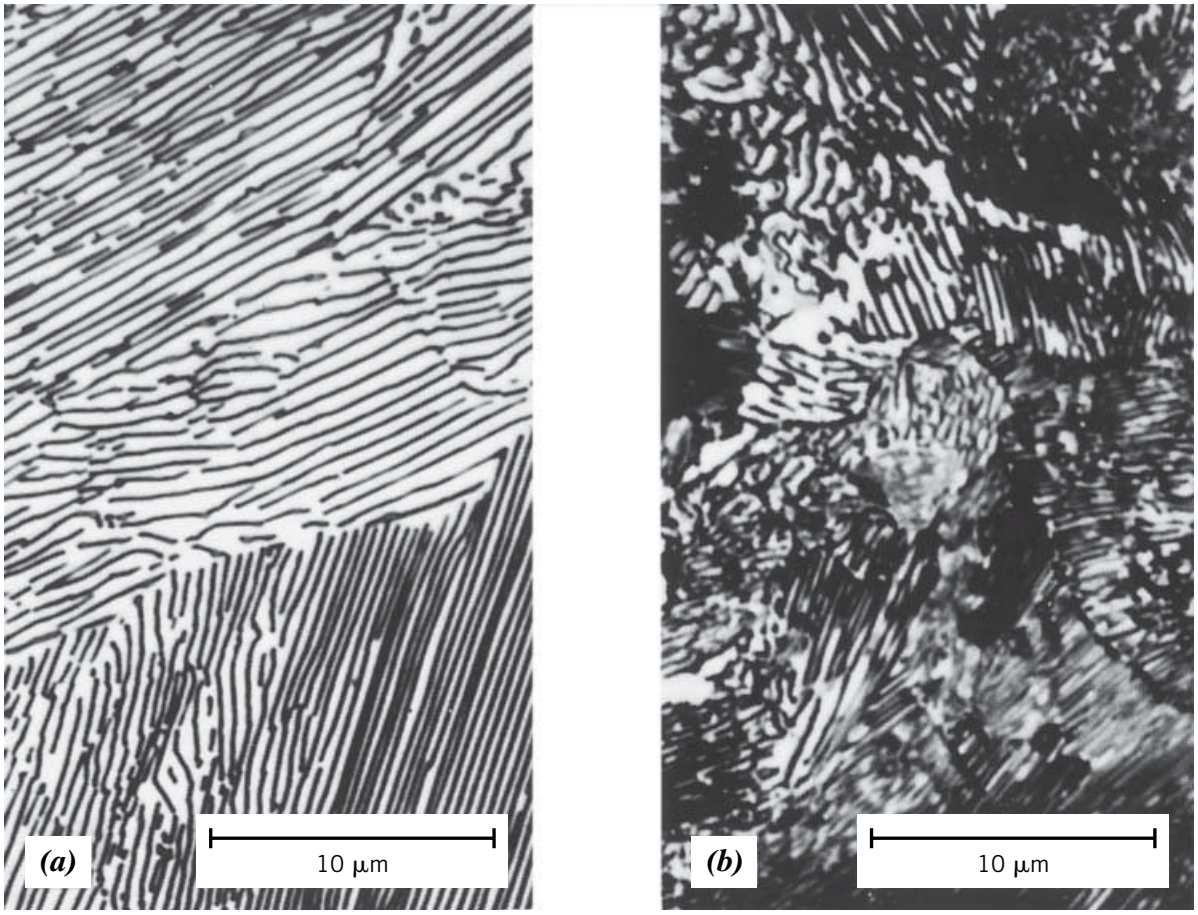

Figure 2: Photomicrographs of (a) coarse pearlite and (b) fine pearlite $\times 3000$ (Callister & Rethwisch, 2018).

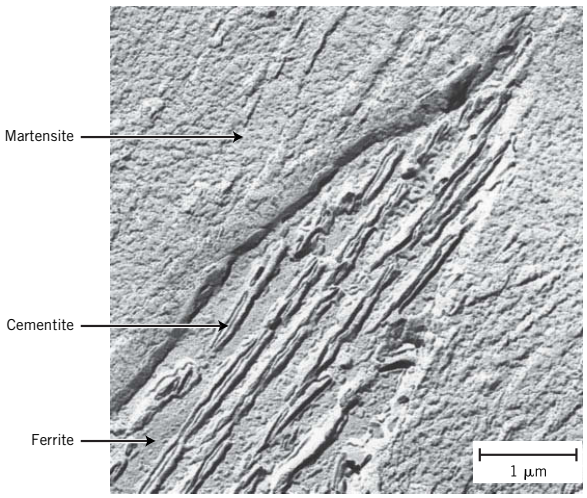

Figure 3: Transmission electron micrograph showing the structure of bainite. A grain of bainite passes from lower left to upper right corners; it consists of elongated and needle-shape particles of Fe_3C within a ferrite matrix. The phase surrounding the bainite is martensite (Callister & Rethwisch, 2018).

Figure 4: Photomicrograph showing the martensitic microstructure. The needleshape grains are the martensite phase, and the white regions are austenite that failed to transform during the rapid quench $\times 1220$ (Callister & Rethwisch, 2018).

References

Asgharzadeh, A., Tiji, S. A. N., Esmaeilpour, R., Park, T., & Pourboghrat, F. (2020). Determination of hardness-strength and-flow behavior relationships in bulged aluminum alloys and verification by fe analysis on rockwell hardness test. *The International Journal of Advanced Manufacturing Technology*, 106(1), 315–331.

Avallone, E. A., Baumeister III, T., & Sadegh, A. (2007). *Marks' standard handbook for mechanical engineers*. McGraw-Hill Education.

Barbato, G., Galetto, M., Germak, A., & Mazzoleni, F. (1998). Influence of the indenter shape in rockwell hardness test. *Proc. of the HARDMEKO '98, Sept*, (pp. 21–23).

Callister, W. D. & Rethwisch, D. G. (2018). *Materials science and engineering: an introduction*, volume 9. Wiley New York.

Low, S., Pitchure, D. J., & Flanigan, C. (2000). The effect of suggested changes to the rockwell hardness test method. In *Proceeding of 16th World Congress of International Measurement Confederation (IMEKO-XVI)*.

Low III, S. R. et al. (2001). Nist recommended practice guide: Rockwell hardness measurement of metallic materials.

Nunura, C. R., dos Santos, C. A., & Spim, J. A. (2015). Numerical–experimental correlation of microstructures, cooling rates and mechanical properties of aisi 1045 steel during the jominy end-quench test. *Materials & Design*, 76, 230–243.

Pimenta, C. D., Silva, M. B., de Morais Campos, R. L., & de Campos Junior, W. R. (2018). Desirability and design of experiments applied to the optimization of the reduction of decarburization of the process heat treatment for steel wire sae 51b35. *American Journal of Theoretical and Applied Statistics*, 7(1), 35–44.